Structure-Based Design of Some MgrA Staphylococcus Aureus Inhibitors

David Ebuka Arthur[a],*, Peter Francis Adikwu[b], Michael Abatyough[c], Ayuba J. Maina[a], Hadiza A. Dawi[a]
and Mohammed A. Askira[a]

[a]*Department of Pure and Applied Chemistry, University of Maiduguri P.M.B 1069, Borno-Nigeria*
[b]*Department of Chemistry, Ahmadu Bello University, Zaria-Nigeria*
[c]*Chemical Science Department, Bingham University, Karu-Nigeria*

Staphylococcus Aureus is an extremely dangerous infectious pathogen in the healthcare and community setting. Discovery of the right chemotherapies to treat this infection has been difficult due to the high toxicity associated with some of the most effective drugs. Computational chemistry is helping to identify potentially effective drugs to treat this infection. In this study, molecular docking was utilized to examine the effects of 3 different compounds on Staphylococcus aureus and HTH3E. The structure of the ligands was drawn in Chemdraw software and the molecular docking was carried out using Pyrx computational tool. Visualizations of the docking interactions with the target active site were generated *via* Discovery Studio. HTH3E showed the lowest binding affinity with a score of -27.105 kcal mol^{-1}. The results demonstrate that (3-amino-5-hydroxy-2-methyl-1H-pyrrol-1-yl)(5-hydroxy-1H-1λ6-thiophen-3-yl)methyl carbamic acid is a promising lead and therefore further study of this compound is warranted.

INTRODUCTION

S. aureus is a significant infectious agent in healthcare, causing infections of varying severity, from mild to possibly fatal. It is highly virulent due to toxins and other virulence factors. Moreover, the acquisition of antimicrobial-resistant genes has made it difficult to treat infections caused by this bacterium, particularly those caused by methicillin-resistant S. aureus (MRSA) which are usually multidrug-resistant [1, 2]. The circulation of MRSA between health settings and communities has altered the genetic map of the strains in both locations. Docking, an extensively used in silico structure-based technique in pharmaceutical discovery, has been ascertained to predict ligand-target communications on a molecular level, recognize novel helpful molecules, or define structure-activity interactions (SAR) without knowing the chemical composition of other target regulators [3].

Currently, there is no approved medication by the Food and Drug Administration (FDA) or specific scientific treatment for staphylococcus aureus infection. Research into creating a single drug for this purpose is estimated to take between 12 and 24 years [4]. It has been suggested that drug discovery is a lengthy and costly endeavor. Research indicates that prior to 2004, it cost an average of US$800 million to bring a new drug to the market [5]. Earlier reports on a potential therapy for staphylococcus aureus combined protease inhibitor [6] which previously need further evaluation. In Nigeria, the use of a computational approach involving dynamic models has been widely accepted as an indispensable tool in drug design. This study looks to build on the success achieved in the field of staphylococcus aureus, by employing in silico drug design techniques to create novel inhibitor drug candidates with improved activity.

The use of Pyrex, Discovery studio Schrodinger suite,

*Corresponding author. E-mail: eadavid@unimaid.edu.ng

and other computational methods for drug discovery and development of staphylococcus aureus is tremendously cost-effective, time-efficient, and environmentally friendly. Not only can these methods help reduce the burden of animal tests and the production of chemical waste, but they can also reduce the overall costs of drug design and development. With rising computer capabilities, these computational methods offer tremendous potential to speed up the process of drug discovery and development for this dangerous bug, bringing us one step closer to safe and effective treatments [7,8].

METHODS

### Experiment Data Sets and Ligand Preparation

Throughout the study, a workstation system with the following specifications was used: Dual 2.30 GHz CPU, Intel® Core i5-3210M, 6.00GB RAM for this study. Figures 1-3 show the chemical structures of the ligand and their corresponding IUPAC names. The 2D structures of the newly designed drug candidates were drawn with Chemdraw software ultra-version 12.0 and presented in Table 4 along with their IUPAC names, thereafter transformed into 3D structures with the aid of Spartan 14 software [9]. Subsequently, the 3D structures obtained were geometrically optimized with the DFT approach using the Spartan 14 software from Wave Function Inc. The optimized ligands were then saved in the pdb file format as the prepared ligands for the following molecular docking simulations study [10].

Retrieval of Receptor and Preparation Show

The 3D structure of the protein complex (PDB: 2BV6) was downloaded from the Protein Data Bank to prepare the receptor. Heteroatoms and water molecules were manually removed from the downloaded 3D structure of the amino acid, and the modified receptor was saved in pdb file format as shown in Fig. 4 [11].

Gibb's Free Energy Calculations and Virtual Screening

A molecular interaction study was conducted to compute the scoring function and research protein-ligand interactions in predicting the binding affinity and biochemical activity of the ligand [12,13]. To estimate the binding affinity,
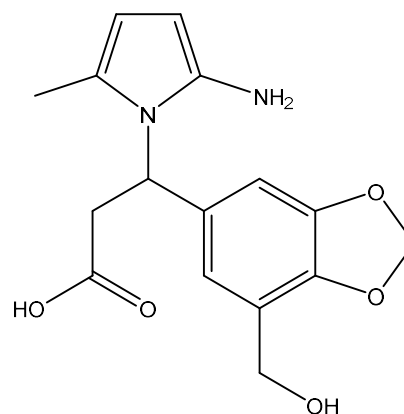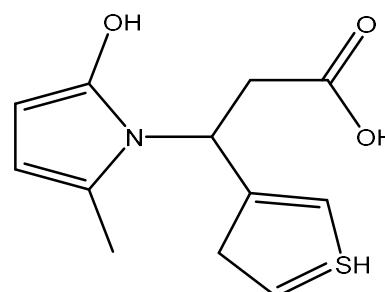

3-(2-amino-5-methyl-1*H*-pyrrol-1-yl)-3-(7-(hydroxymethyl)benzo[*d*][1,3]dioxol-5-yl)propanoic acid

Fig. 1. 2-d structure of the first ligand (HTH1) with its IUPAC name used in the study.
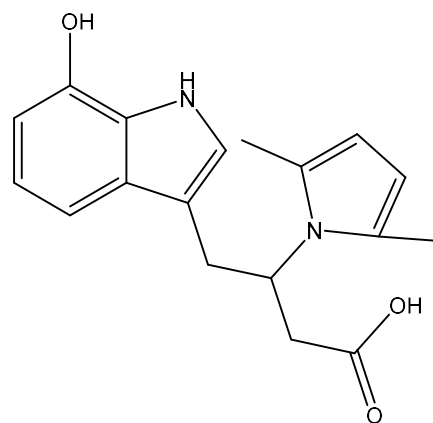
3-(2,5-dimethyl-1*H*-pyrrol-1-yl)-4-(7-hydroxy-1*H*-indol-3-yl)butanoic acid

Fig. 2. 2-d structure of the second ligand (HTH2) with its IUPAC name used in the study.

3-(2-hydroxy-5-methyl-1*H*-pyrrol-1-yl)-3-(3*H*-1λ⁴-thiophen-4-yl)propanoic acid

Fig. 3. 2-d structure of the second ligand (HTH3) with its IUPAC name used in the study.

Fig. 4. 3D structure of the receptor HTH-MgrA (PDB ID: 2BV6) with a resolution of 2.80 Å.

AutoDock Vina 4.2 of PyRx software was used, while visualization of protein-ligand interactions by non-bonding and hydrophobic interactions was explored using the 2016 version of Discovery Studio Visualizer software [14]. Using the virtual screening instrument PyRx, the protein structure (PDB ID: 2BV6) in pdb format was opened and the molecules were converted into pdbqt layout. Afterward, the lattice box was generated along with the choice of both the center of the mark site and its dimensions. The precision of the docking situation was observed through the utilization of autodock Vina.

Molecular Dynamics (MD) with Desmond Simulation Package

The MD simulation was carried out using the Desmond simulation package of Schrödinger LLC [15]. The OPLS_2005 force field parameters were used to simulate an NPT ensemble for 1.2 ns with a relaxation time of 1 ps for the lead inhibitors and the best-designed ligand, at a temperature of 300K and pressure of 1bar [16,17] and the long-range electrostatic interactions were calculated using the Particle Mesh Ewald method [18,19] with a cutoff radius of 9.0 Å. The Simple Point Charge model was used to explicitly describe the water molecules. A Martyna-

Tuckerman-Klein chain with a coupling constant of 2.0ps was employed to maintain pressure control, while a Nose-Hoover chain was used for coupling [20-22] for temperature control.

The stability of the molecular dynamics simulations was evaluated by monitoring the root mean square deviation (RMSD) of the ligand and protein at different points in time. Non-bonded forces were calculated using an r-RESPA integrator, with short-range forces updated every step and long-range forces updated every three steps. Trajectories were saved at 4.8 ps intervals for further analysis with the Simulation Interaction Diagram, implemented in the Desmond MD package, to analyze the behavior and interactions between the ligands and protein. The AMBER 14 package [23] with the AMBER force field ff99 [24] was also used to minimize, add counter ions, solvate, equilibrate, and run periodic box, explicit water (TIP4P) MD simulations for the best inhibitors. The protein-ligand-water system data analysis was carried out with the AMBER Tools distribution program [25,26]

RESULT AND DISCUSSION

The molecular docking result of all three compounds and the newly designed ones are presented in Table 1 below. Table 1 shows the binding score, hydrogen bond, hydrophobic interaction, solvation energy, and dissolved solvent, all calculated in kcal mol^{-1}, for the ligands used in a molecular docking study of the Mgra receptor.

Table 1 reveals that HTH3E has the least binding score of -27.105 kcal mol^{-1} but has the best binding affinity among all compounds. HTH1E has a binding score of -13.071 kcal mol^{-1} and hydrogen bond energy of -8.873 kcal mol^{-1}; HTH1F has a binding score of -13.701 kcal mol^{-1} and hydrogen bond energy of -7.873 kcal mol^{-1}; Whereas, HTH1B has a higher binding score of -10.64 kcal mol^{-1}, but its hydrogen bond energy is only -3.279 kcal mol^{-1}, thus making it a more effective Mgra inhibitor than HTH1E and HTH1F.

In 2019, the best-known Mgra inhibitor was 3-(2-amino-5-methyl-1H-pyrrol-1-yl)-3-(7-hydroxymethyl) benzol (d) (1,3) dioxol(-5,yl) propanoic acid, which was docked with a pre-prepared 1T64 protein grid and energy-optimized pharmacophore. It had a binding score of -25.145 kcal mol^{-1},

Table 1. Quantitative Description of the Interaction of HTH1, HTH2, HTH3 and their Analogues on HTH-MgrA Receptor (PDB ID: 2BV6)

Name	Score	Nflex	Hbond	Hphob	Vwlnt	Eintl	Dsolv	SolEI
HTH1	-25.145	5	-5.764	-4.249	-20.836	5.830	10.741	3.129
HTH1A	-22.578	7	-6.820	-3.679	-19.537	6.326	14.281	2.676
HTH1B	-10.640	8	-3.279	-3.671	-20.159	6.262	15.539	5.789
HTH1C	-19.058	9	-6.737	-3.701	-18.976	11.700	16.487	2.542
HTH1D	-14.199	9	-5.781	-2.983	-18.199	3.836	19.478	0.935
HTH1E	-13.071	9	-8.879	-3.153	-14.995	11.288	24.012	4.682
HTH1F	-13.701	10	-7.873	-3.190	-17.673	8.640	23.849	3.244
HTH2	-20.380	6	-4.750	-4.321	-21.130	4.270	12.084	4.548
HTH2A	-16.209	6	-3.718	-4.404	-21.751	3.818	13.482	6.346
HTH2B	-23.552	6	-8.450	-3.999	-19.792	9.151	16.247	6.834
HTH2C	-17.763	5	-4.271	-4.375	-19.381	1.371	13.419	3.471
HTH2D	-15.941	5	-5.572	-3.576	-18.880	3.804	15.223	7.597
HTH2E	-15.874	5	-5.629	-3.371	-23.241	5.541	20.061	8.818
HTH2F	-16.679	6	-5.256	-3.780	-17.895	5.029	14.068	4.386
HTH3	-15.173	5	-3.539	-4.348	-17.725	2.993	10.145	5.775
HTH3A	-16.910	5	-4.956	-3.865	-18.110	2.295	11.969	6.591
HTH3B	-13.205	5	-4.015	-2.946	-16.939	2.212	13.418	4.245
HTH3C	-15.705	5	-4.996	-2.851	-17.480	2.915	13.724	4.595
HTH3D	-16.246	5	-8.029	-2.376	-13.833	5.904	16.867	5.822
HTH3E	-27.105	5	-8.549	-2.958	-20.299	5.662	15.707	3.068

Nflex: - Number of rotatable torsions. Hbond: - hydrogen bond energy. Hphob: - hydrophobic energy in exposing a surface to water. Vwint: - The van der Waals interaction energy (sum of gc and gh van der Waals). Eintl: - Internal conformational energy of the ligand. Dsolv: - The desolvation of exposed H-bond donors and acceptors. SolEl: - The solvation electrostatics energy change upon binding.

which was higher than that of HTH3E, making it the better inhibitor [27].

Figure 5 provides a 3D and 2D view of the interaction types between amino acids in 2BV6 and the HTH1 receptor. Table 2 outlines the results of the interaction types along with the amino acids involved. The first bond has a distance of 1.71 and involves a conventional hydrogen bond between the hydrogen donor AGR86: HH and the hydrogen acceptor HTH1. At a distance of 4.15, a H donor bond is formed between HTH1's sulfur atom and the pi orbitals of VAL69. A distance of 4.92 has a pi orbitals bond between AGR92 and HTH1's pi orbitals. Lastly, the bond at 5.07 consists of a

pi-alkyl bond from HTH1's pi orbitals to VAL59's alkyl. This interaction type helps us understand the communication between the amino acids of 2BV6 and the HTH1 receptor.

The hydrogen bond binding score and the hydrogen bond energy of HTH1 are highlighted in Table 1 showing -25.145 kcal mol^{-1} and -5.764 kcal mol^{-1} respectively. Stabilizing energy, responsible for the binding affinity of HTH1 is due to the presence of hydrogen bonds between the ligands and the receptor. This is shown in Table 2. Additional contributors to the interaction energy are the pi-orbital and Pi-Alkyl interactions. These help in forming a secure bond between the ligands and the hydrogen bond. In simple terms,
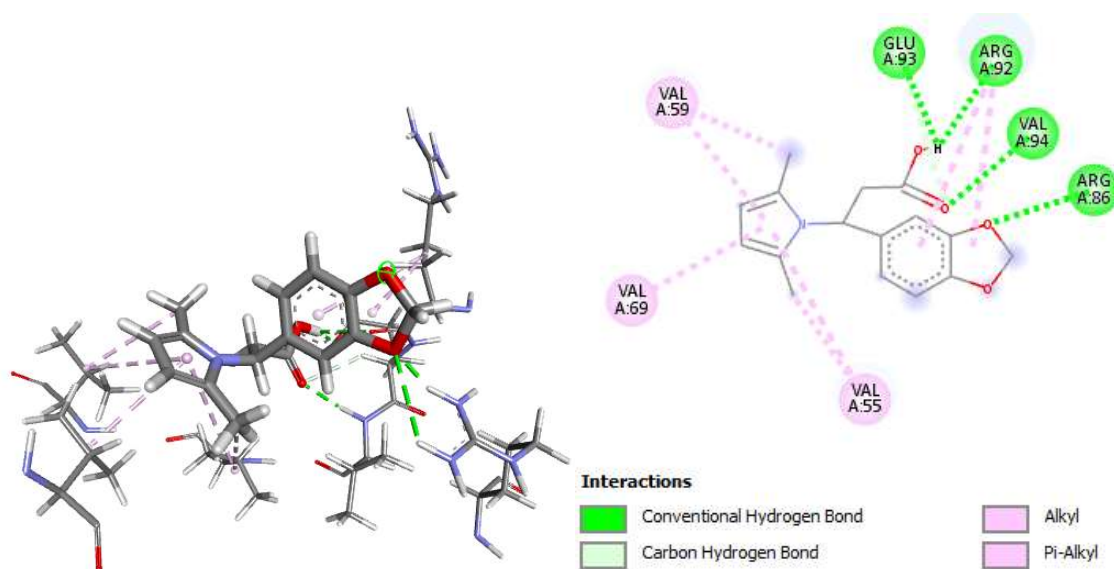
Fig. 5. 2D and 3D view of interaction type of HTH1 with surrounding amino acids of 2BV6.

Table 2. Interaction Types and Amino Acids Involved in the Inhibition of HTH-MgrA Receptor (PDB ID: 2BV6) with HTH1 Inhibitor

Bond distance	Bond type	Bond donor species	Bond donor type	Bond donor acceptor species	Bond acceptor type
1.71	Conventional hydrogen bond	A:ARG86:HH12	H-Donor	:HTH1:O1	H-Acceptor
2.98	Conventional hydrogen bond	A:ARG86:HH22	H-Donor	:HTH1:O1	H-Acceptor
2.14	Conventional hydrogen bond	A:VAL94:HN	H-Donor	:HTH1:O3	H-Acceptor
2.93	Conventional hydrogen bond	:HTH1:H9	H-Donor	A:ARG92:O	H-Acceptor
2.20	Conventional hydrogen bond	:HTH1:H9	H-Donor	A:GLU93:OE1	H-Acceptor
2.81	Carbon hydrogen bond	A:GLU93:HA	H-Donor	:HTH1:O3	H-Acceptor
4.36	Alkyl	A:ARG92	Alkyl	:HTH1	Alkyl
4.22	Alkyl	:HTH1:C15	Alkyl	A:VAL59	Alkyl
4.70	Alkyl	:HTH1:C16	Alkyl	A:VAL55	Alkyl
5.49	Pi-Alkyl	:HTH1	Pi-Orbitals	A:VAL55	Alkyl
5.07	Pi-Alkyl	:HTH1	Pi-Orbitals	A:VAL59	Alkyl
4.15	Pi-Alkyl	:HTH1	Pi-Orbitals	A:VAL69	Alkyl
4.92	Pi-Alkyl	:HTH1	Pi-Orbitals	A:ARG92	Alkyl

these factors together are responsible for the intricate interaction between the ligands with the hydrogen bond as well as the overall binding affinity of HTH1.

Figure 6 and Fig. 3 display the 3D and 2D views of the

interaction type of HTH1A, a hydrogen acceptor, with its surrounding amino acids in the Mgra receptor (PDB ID: 2BV6). Table 3 further outlines the result of the interaction and the amino acids involved in this interaction. There are
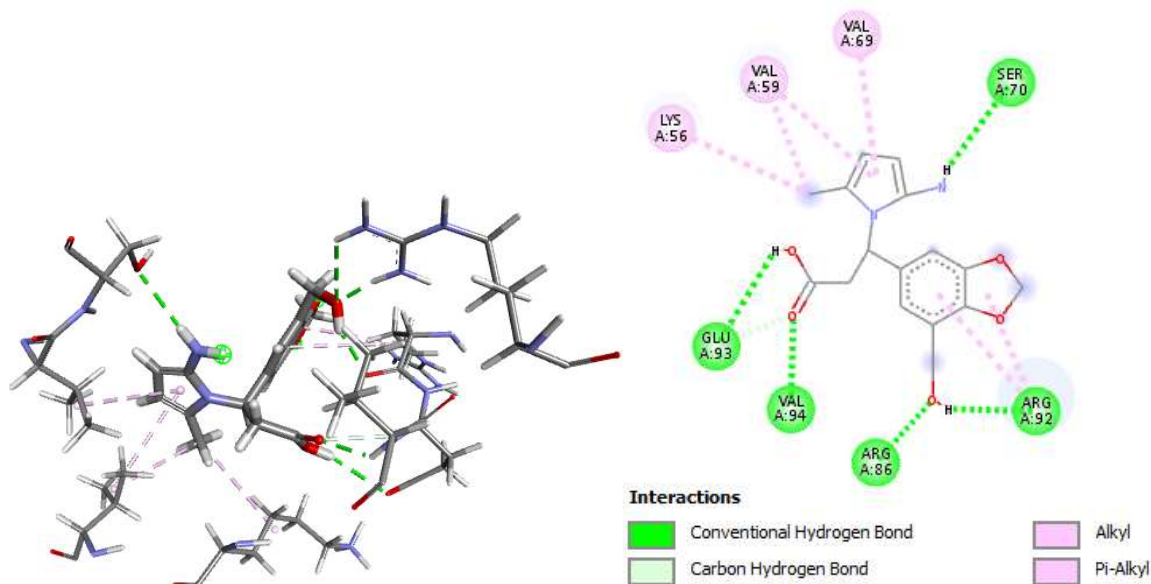
Fig. 6. 2D and 3D view of interaction type of HTH1A with surrounding amino acids of 2BV6.

Table 3. Interaction Types and Amino Acids Involved in the Inhibition of HTH-MgrA Receptor (PDB ID: 2BV6) with HTH1A Inhibitor

Bond distance	Bond type	Bond donor species	Bond donor type	Bond acceptor species	Bond acceptor type
1.60	Conventional hydrogen bond	A:ARG86:HH12	H-Donor	:HTH1A:O3	H-Acceptor
2.95	Conventional hydrogen bond	A:ARG86:HH22	H-Donor	:HTH1A:O3	H-Acceptor
2.03	Conventional hydrogen bond	A:VAL94:HN	H-Donor	:HTH1A:O4	H-Acceptor
2.17	Conventional hydrogen bond	:HTH1A:H12	H-Donor	A:ARG92:O	H-Acceptor
2.51	Conventional hydrogen bond	:HTH1A:H13	H-Donor	A:GLU93:OE1	H-Acceptor
2.59	Conventional hydrogen bond	:HTH1A:H14	H-Donor	A:SER70:OG	H-Acceptor
2.75	Carbon hydrogen bond	A:GLU93:HA	H-Donor	:HTH1A:O4	H-Acceptor
4.28	Alkyl	A:ARG92	Alkyl	:HTH1A	Alkyl
4.69	Alkyl	:HTH1A:C16	Alkyl	A:LYS56	Alkyl
4.07	Alkyl	:HTH1A:C16	Alkyl	A:VAL59	Alkyl
4.90	Pi-Alkyl	:HTH1A	Pi-Orbitals	A:ARG92	Alkyl
4.48	Pi-Alkyl	:HTH1A	Pi-Orbitals	A:VAL59	Alkyl
4.53	Pi-Alkyl	:HTH1A	Pi-Orbitals	A:VAL69	Alkyl

four types of bonds formed between HTH1A and the other amino acids. At a distance of 1.60 Å is a conventional hydrogen bond from the hydrogen donor (A: AGR86:HH12) to the hydrogen acceptor (: HTH1A). The type of bond formed at a distance of 2.95 Å is an H donor (: HTH1A: S)

to Alkyl (A: LYS56). At a distance of 2.03 Å the type of bond formed is pi orbitals (A: VAL94) to H donor (: HTH1A). Lastly, the type of bond formed at a distance of 4.53 Å is pi-orbitals (HTH1A) to Pi Alkyl (A: VAL69). All these bonds are essential for the proper functioning of the Mgra receptor

protein and further gain insight into its structure and function.

The binding score and hydrogen bond of HTH1A are shown in Table 1, indicating a specific binding affinity with -22.578 kcal mol^{-1} and -6.820 kcal mol^{-1}, respectively. This binding score is mainly attributed to the presence of conventional hydrogen bonds between the ligands and the receptor. Additionally, Table 3 displays other forms of stabilization energy associated with the binding affinity of

HTH1A such as from pi-orbital and Pi-Alkyl interactions of the ligands with the hydrogen bond interaction within the complex. These interactions are essential as they can ultimately help to stabilize the overall binding score between the receptor and ligands.

The chemical structures of the newly designed compounds along with their IUPAC names are presented in Table 4.

Table 4. Chemical Structures of the Newly Designed Compounds

HTH3		3-(2,5-Dimethyl-H-pyrrol-1-yl)-3-(2H-1λ^4 thiophen-3-yl) propanoic acid
HTH3A		3-(2-Hydroxy-5-methyl-1H-pyrrol-1-yl)-3-(3H-1λ^4-thiophen-4-yl)propanoic acid
HTH3B		3-(2,5-Dihydroxy-1H-pyrrol-1-yl)-3-(3H-λ^4-thiophen-4-yl)propanoic acid
HTH3C		(2,5-Dihydroxy-1H-pyrrol-1-yl)(thiophen-3-yl)methyl)carbamic acid
HTH3D	((3-amino-2,5-dihydroxy-1*H*-pyrrol-1-yl)(thiophen-3-yl)methyl)carbamic acid	(3-Amino-2,5-dihydroxy-1H-pyrrol-1-yl)(thiophen-3-yl)methyl)carbamic acid
HTH3E		(3-Amino-5-hydroxy-2-methyl-1H-pyrrol-1-yl)(5-hydroxy-1H-1λ^6-thiophen-3-yl)methyl carbamic acid

Table 4. Continued

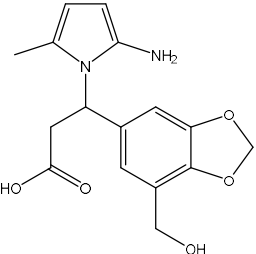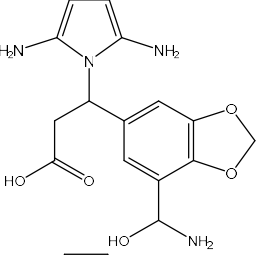|		
HTH3F		(3,4-Diamino-2,5-dihydroxy-1H-pyrrol-1-yl)(5-hydroxythiophen-3-yl)methyl carbamic acid
HTH2		3-(2,5-Dimethyl-H-pyrrol-1-yl)-4-(7-hydroxy-1H-indol-3-yl)butanoic acid
HTH2A		3-(2,5-Dimethyl;-1H-pyrrol-1-yl)-4(7-hydroxy-1H-indol-3-yl)butanoic acid
HTH2B		4-(7-Hydroxy-4-indol-3-yl)-3-(2-hydroxy-5-methyl-1H-pyrrol-1-yl)butanoic acid
HTH2C		3-((7-Hydroxy-1H-indol-3-yl)amino)-3-(2-hydroxy-5-methyl-1H-pyrrol-1-yl)propanoic
HTH2D		3-((7-Hydroxy-1H-pyrrolo(3,2-b)pyridine-3-yl)amino)-3-(2-hydroxy-5-meyhyl-1H-pyrrol-1-yl)propanoic acid
HTH2E		3-(3,5-Dihydroxy-2-methyl-1H-pyrrol-1yl-)-3-(7-hydroxy-1H-pyrrolo(3,2)-b)pyridine-3-yl)amino)propanoic acid

Table 4. Continued
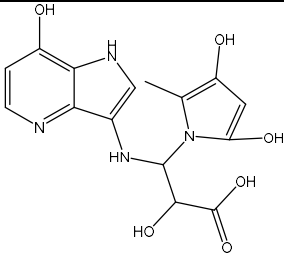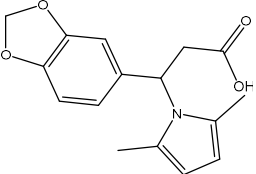
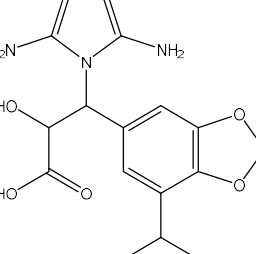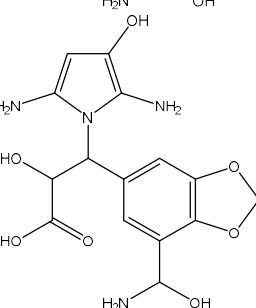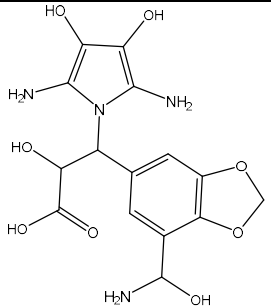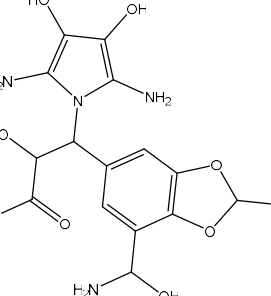| HTH2F		3-(3,5-Dihydroxy-2-methyl-1H-pyrrol-1-yl)-2-hydroxy-3-((7-hydroxy-1H-pyrrolo(3,2-b)pyridin-3-yl)amino)propanoic acid
HTH1		3-(2-Amino-5-methyl-1H-pyrrol-1-yl)-3-(7hydroxymethyl)(d)1,3)dioxol-5-propanoic acid
HTH1A		3-(2-Amino-5-methyl-1H-pyrrpl-1-yl-3-(7-hydroxymethyl)benzo(d)(1,3)-5-yl)propanoic acid
HTH1B		3-(7-(Amino(hydroxyl)methyl)benzo(d)(1,3)dioxol-5-yl)-3-(2,5)diamino-1H-pyrrol-1-yl)propanoic acid
HTH1C		3-(7-(Amino(hydroxyl)methyl)benzo(d)(1,3)dioxol-5-yl)-3-(2,5-diamino-1H-pyrrol-1-yl)-2-hydroxy propanoic acid
HTH1D		3-(7-(Amino(hydroxyl)methyl)benzo(d)(1,3)dioxol-5-yl)-3-(2,5-diamino-3-hydroxy-1H-pyrrol-1-yl)-2-hydroxypropanoic acid

Table 4. Continued

HTH1E		3-(7-(Amino(hydroxyl)methyl)benzo(d)(1,3)dioxol-5-5yl)-3-3(2,5diamino-3-4-dihydroxy-1H-pyrrol-1-yl)-2-hydroxypropanoic acid
HTH1F		3-(7-(Amin0(hydroxyl)methyl)-2-hydroxybenzo(d) (1,3)dioxol-5-yl)-3-(2,5-diamino-3,4-dihydroxy-1H-pyrrol-1-yl)-2-hydroxypropanoic acid

Figure 7 and Fig. 5 illustrate the 3D and 2D views of interactions between HTH2 and the surrounding amino acids of the Mgra receptor (PDB ID: 2BV6). Table 5 provides further details of these interactions and the amino acids involved. The types of bonds formed and the distances at which these occur are also shown. At a distance of 2.5, a conventional hydrogen bond is formed between the hydrogen donor (A: AGR86: HH12) and the hydrogen acceptor (: HTH2). At a distance of 1.69, an H donor (: HTH2: S) to Alkyl (A: val69) bond is produced. At a distance of 1.94, pi orbitals (A: GLU93) to H donor (: HTH2) bond is formed while at a distance of 3.00, a pi lone pair (HTH2) to Pi Alkyl (A: ARG92) bond occurs. These details provide us with insights into how the underlying dynamics of receptor-ligand interactions play out to facilitate biochemical processes.

Table 1 indicates that the binding score and hydrogen bond of HTH2 are -20.380 kcal mol^{-1} and -4.750 kcal mol^{-1} respectively. The binding affinity of HTH2 is primarily provided by the presence of conventional hydrogen bonds between the ligands and the receptor, leading to increased interaction energy. Further stabilization is imparted by additional energy interactions, such as pi-lone pairs and pi-alkyl interactions. These interactions increase the binding affinity and hydrogen bonds within the complex,

while the Table 5 illustrates the approximate magnitude of such interactions. Taken together, energy interactions between the ligands and receptors are vital in determining the binding affinity of HTH2.

Figure 8 and Table 6 both illustrate the interactions between HTH2B and surrounding amino acids of the Mgra receptor, PDB ID: 2BV6. The 3D view of Fig. 8 clearly reveals the bonds established between HTH2B and the Amino acids at varying distances. Table 6 further provides a comprehensive overview of all the bonds formed, their types, and the amino acids involved in the process. For example, a conventional hydrogen bond is formed between the hydrogen donor (A: GLY67: HN) and the hydrogen acceptor (: HTH2B) at a distance of 2.52 Å. Furthermore, a Hydrogen donor (: HTH2:S) to Alkyl bond (A: ARG86HN12) is formed at a distance of 1.75 Å while a Pi orbitals bond (A: ARGHH22) to H donor (: HTH2B) is formed at a distance of 1.74 Å. Lastly, the type of bond formed at a distance of 2.94 Å is hydrogen donor (HTH2) to Pi Alkyl (A: ASN54). In conclusion, Fig. 8 and Table 6 accurately represent the intricate relationship between HTH2B and the surrounding Amino acids of the receptor.

The binding score and the hydrogen bond of HTH2B are two important components that determine the affinity
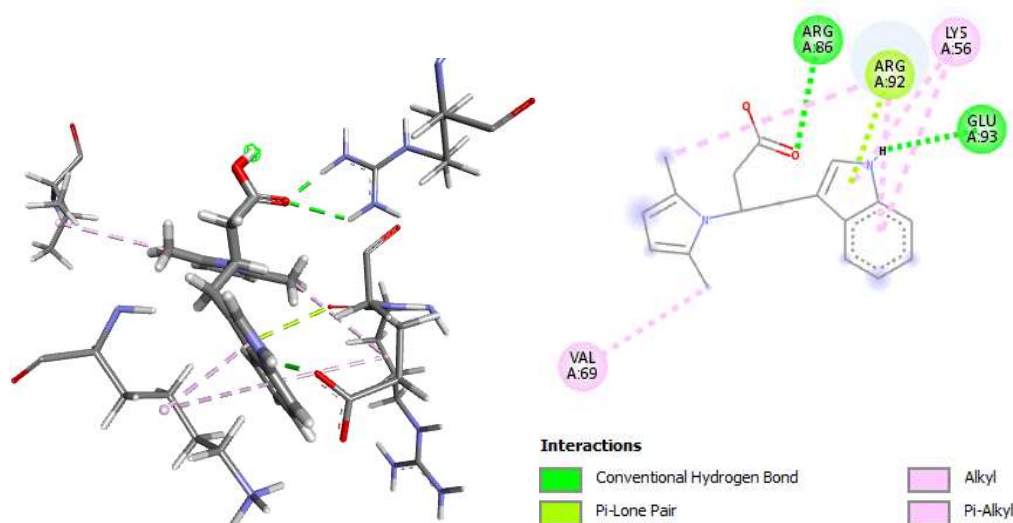
Fig. 7. 2D and 3D view of interaction type of HTH2 with surrounding amino acids of 2BV6.

Table 5. Interaction Types and Amino Acids Involved in the Inhibition of HTH-MgrA Receptor (PDB ID: 2BV6) with HTH2 Inhibitor

Bond Distance	Bond type	Bond donor type	Bond donor species	Bond acceptor species	Bond acceptor type
2.52	Conventional hydrogen bond	A:ARG86:HH12	H-Donor	:HTH2:O1	H-Acceptor
1.96	Conventional hydrogen bond	A:ARG86:HH22	H-Donor	:HTH2:O1	H-Acceptor
1.94	Conventional hydrogen bond	:HTH2:H16	H-Donor	A:GLU93:OE1	H-Acceptor
3.00	Pi-Lone Pair	A:ARG92:O	Lone Pair	:HTH2	Pi-Orbitals
4.33	Alkyl	:HTH2:C10	Alkyl	A:VAL69	Alkyl
4.95	Alkyl	:HTH2:C9	Alkyl	A:ARG92	Alkyl
4.32	Pi-Alkyl	:HTH2	Pi-Orbitals	A:LYS56	Alkyl
5.42	Pi-Alkyl	:HTH2	Pi-Orbitals	A:LYS56	Alkyl
4.32	Pi-Alkyl	:HTH2	Pi-Orbitals	A:ARG92	Alkyl

between the receptor and its ligand. The binding score of HTH2B was determined to be -23.552 kcal mol^{-1} and the hydrogen bond was -8.450 kcal mol^{-1}, as indicated in Table 1. It has been established that the presence of conventional hydrogen bonds between the ligands and the binding score of the receptor is primarily responsible for the addition of the interaction energy. Moreover, Table 6 displays these interactions between the receptor and its ligand. Stabilizing energy of the HTH2B is also attributed to H donor and Pi-Alky interactions, which are responsible for

the hydrogen bonding within the complex. Therefore, the binding score and hydrogen bond of HTH2B are two critical factors that contribute to the energy of the binding affinity. which further enhances the interaction energy of the complex. This result was found to be similar to those reported by Khan et al. in 2021, as well as Arthur et al. in 2022 where the high docking score reported was correlated to the number of hydrogen bonds formed between the ligands and the receptor [8,10].
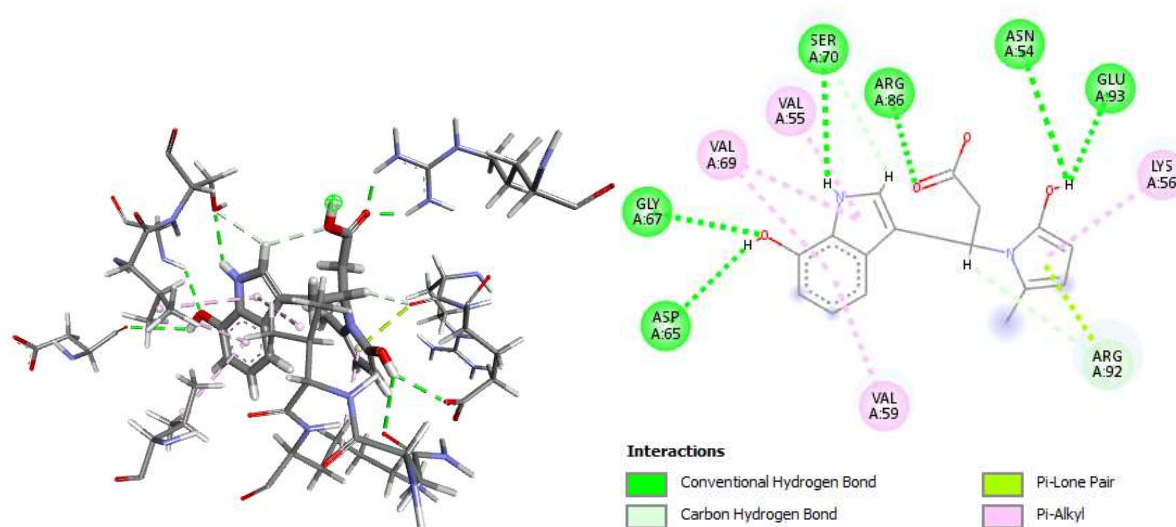
Fig. 8. 2D and 3D view of interaction type of HTH2B with surrounding amino acids of 2BV6.

Table 6. Interaction Types and Amino Acids Involved in the Inhibition of HTH-MgrA Receptor (PDB ID: 2BV6) with HTH2B Inhibitor

Bond distance	Bond type	Bond donor species	Bond donor type	Bond acceptor species	Bond acceptor type
2.52	Conventional hydrogen bond	A:GLY67:HN	H-Donor	:HTH2B:O3	H-Acceptor
1.75	Conventional hydrogen bond	A:ARG86:HH12	H-Donor	:HTH2B:O4	H-Acceptor
1.74	Conventional hydrogen bond	A:ARG86:HH22	H-Donor	:HTH2B:O4	H-Acceptor
2.94	Conventional hydrogen bond	:HTH2B:H17	H-Donor	A:ASN54:OD1	H-Acceptor
2.36	Conventional hydrogen bond	:HTH2B:H17	H-Donor	A:GLU93:OE1	H-Acceptor
2.83	Conventional hydrogen bond	:HTH2B:H18	H-Donor	A:ASP65:O	H-Acceptor
2.37	Conventional hydrogen bond	:HTH2B:H5	H-Donor	A:SER70:OG	H-Acceptor
2.76	Carbon hydrogen bond	:HTH2B:H4	H-Donor	A:SER70:OG	H-Acceptor
2.67	Carbon hydrogen bond	:HTH2B:H4	H-Donor	:HTH2B:O1	H-Acceptor
2.79	Carbon hydrogen bond	:HTH2B:H8	H-Donor	A:ARG92:O	H-Acceptor
2.89	Pi-Lone Pair	A:ARG92:O	Lone Pair	:HTH2B	Pi-Orbitals
4.15	Pi-Alkyl	:HTH2B	Pi-Orbitals	A:VAL59	Alkyl
4.56	Pi-Alkyl	:HTH2B	Pi-Orbitals	A:VAL69	Alkyl
5.17	Pi-Alkyl	:HTH2B	Pi-Orbitals	A:VAL55	Alkyl
4.26	Pi-Alkyl	:HTH2B	Pi-Orbitals	A:VAL69	Alkyl
4.64	Pi-Alkyl	:HTH2B	Pi-Orbitals	A:LYS56	Alkyl

Figure 9 and Fig. 6 depict the 3D and 2D view respectively of the interaction type between the Human Transcription Factor-3 (HTH3) and the surrounding amino acids of 2BV6, a receptor encoded by the Mgra gene. Table 7 provides the results of the interaction type and nine surrounding amino acid residues, which are involved in
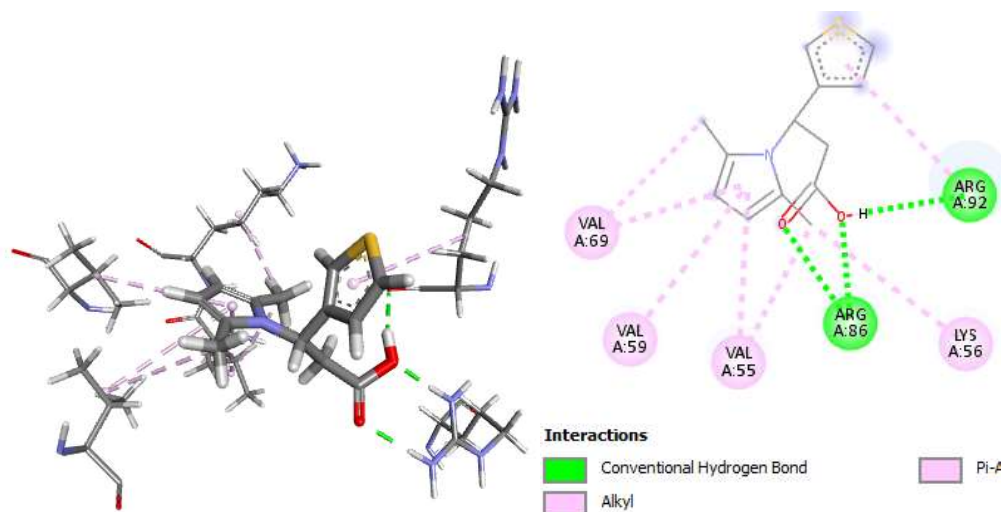
Fig. 9. 2D and 3D view of interaction type of HTH3 with surrounding amino acids of 2BV6.

Table 7. Interaction Types and Amino Acids Involved in the Inhibition of HTH-MgrA Receptor (PDB ID: 2BV6) with HTH3 Inhibitor

Bond distance	Bond type	Bond donor species	Bond donor type	Bond acceptor Species	Bond acceptor type
1.62	Conventional hydrogen bond	A:ARG86:HH12	H-Donor	:HTH3:O2	H-Acceptor
1.90	Conventional hydrogen bond	A:ARG86:HH22	H-Donor	:HTH3:O1	H-Acceptor
2.13	Conventional hydrogen bond	:HTH3:H12	H-Donor	A:ARG92:O	H-Acceptor
4.67	Alkyl	:HTH3:C5	Alkyl	A:VAL69	Alkyl
4.05	Alkyl	:HTH3:C6	Alkyl	A:VAL55	Alkyl
4.41	Alkyl	:HTH3:C6	Alkyl	A:LYS56	Alkyl
4.84	Pi-Alkyl	:HTH3	Pi-Orbitals	A:VAL55	Alkyl
5.10	Pi-Alkyl	:HTH3	Pi-Orbitals	A:VAL59	Alkyl
5.02	Pi-Alkyl	:HTH3	Pi-Orbitals	A:VAL69	Alkyl
4.89	Pi-Alkyl	:HTH3	Pi-Orbitals	A:ARG92	Alkyl

forming four different types of bonds. These include conventional hydrogen bond at a distance of 1.62 Angströms, H donor to Alkyl at 1.90 Å, pi orbital to H donor at 4.41 Å and H donor to Pi Alkyl at 4.84 Å. All these interactions revealed by the 3D and 2D visualizations, as well as Table 7, contribute to the overall conformation and appearance of the Mgra-encoded receptor 2BV6 and in turn, the behavior of the receptor with its ligands.

The binding score and hydrogen bond of HTH3, as indicated in Table 1 (-15.173 kcal mol^{-1} and -3.539 kcal mol^{-1}), were mainly responsible for the addition of the interaction energy. Table 7 shows this interaction in greater detail. Other energies that contribute to the binding affinity of HTH3 come from the H-donor and Pi-Alkyl interactions within the complex alongside the hydrogen bond interaction.

Figure 10 shows the 3D view of the interaction type of HTH3 with the surrounding amino acids of 2BV6 and the 2D view of the interaction type of HTH3E with the surrounding amino acids of 2BV6. Table 8 shows the results of the
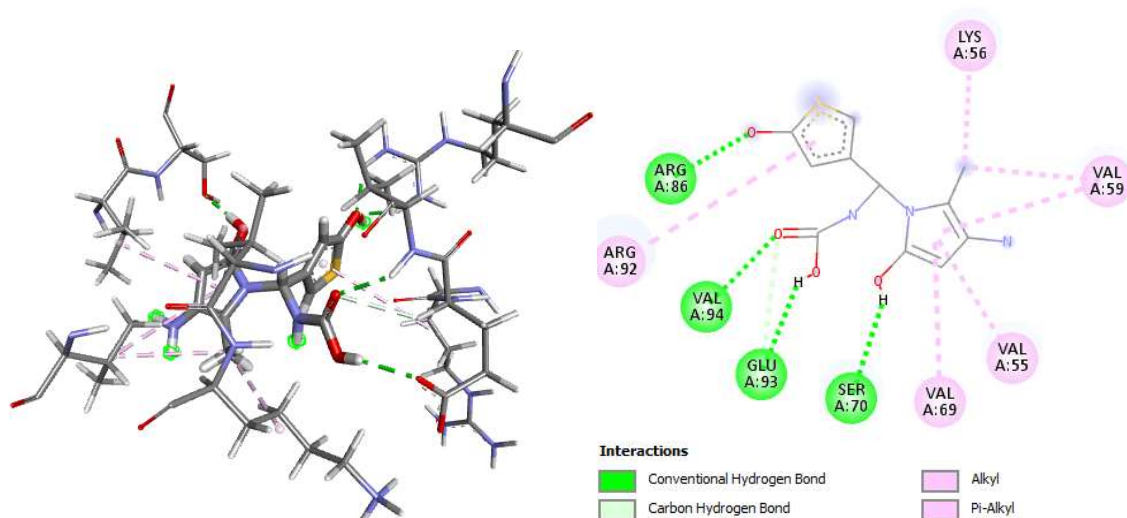
Fig. 10. 2D and 3D view of interaction type of HTH3E with surrounding amino acids of 2BV6.

Table 8. Interaction Types and Amino Acids Involved in the Inhibition of HTH-MgrA Receptor (PDB ID: 2BV6) with HTH3E Inhibitor

Bond distance	Bond type	Bond donor species	Bond donor type	Bond acceptor species	Bond acceptor type
1.87	Conventional hydrogen bond	A:ARG86:HH12	H-Donor	:HTH3E:O4	H-Acceptor
2.04	Conventional hydrogen bond	A:ARG86:HH22	H-Donor	:HTH3E:O4	H-Acceptor
2.23	Conventional hydrogen bond	A:VAL94:HN	H-Donor	:HTH3E:O2	H-Acceptor
2.07	Conventional hydrogen bond	:HTH3E:H10	H-Donor	A:SER70:OG	H-Acceptor
2.19	Conventional hydrogen bond	:HTH3E:H4	H-Donor	A:GLU93:OE1	H-Acceptor
2.88	Carbon hydrogen bond	A:GLU93:HA	H-Donor	:HTH3E:O2	H-Acceptor
4.55	Alkyl	:HTH3E:C11	Alkyl	A:LYS56	Alkyl
4.24	Alkyl	:HTH3E:C11	Alkyl	A:VAL59	Alkyl
5.49	Pi-Alkyl	:HTH3E	Pi-Orbitals	A:VAL55	Alkyl
5.08	Pi-Alkyl	:HTH3E	Pi-Orbitals	A:VAL59	Alkyl
4.25	Pi-Alkyl	:HTH3E	Pi-Orbitals	A:VAL69	Alkyl
5.47	Pi-Alkyl	:HTH3E	Pi-Orbitals	A:ARG92	Alkyl

interaction type and the amino acids involved in the Mgra receptor (PDB ID: 2BV6). At a distance of 1.87, there is a conventional hydrogen bond from the hydrogen donor (A: ARG86:HH12) to the hydrogen acceptor (HTH3E). At a distance of 2.04, there is an H donor (HTH3E:S) to an Alkyl (A: ARG86:HH22). At a distance of 2.23, the type of bond formed is a pi orbital (A: VAL94) to an H donor (HTH3E).

Lastly, at a distance of 2.07, the type of bond formed is an H donor (HTH3E) to a Pi Alkyl (A: VAL69).

The binding score and hydrogen bond of HTH3E were primarily responsible for the addition of interaction energy and are indicated in Table 1 as -27.105 kcal mol^{-1} and -8.549 kcal mol^{-1}, respectively. Stabilizing energy associated with the binding affinity of HTH3E, including H-donor and

Pi-alkyl interactions, was facilitated by the hydrogen bond interaction within the complex, as shown in Table 8. The result of the molecular dynamics study of the HTH3E compound is presented as follows.

The Root Mean Square Deviation (RMSD) is used to measure the average change in displacement of a selection of atoms for a particular frame with respect to a reference frame. It is calculated for all frames in the trajectory.

Figure 11 illustrates the RMSD evolution of a protein (left Y-axis). All protein frames are aligned on the reference frame backbone and the RMSD is calculated based on the selected atoms. This information is useful in determining the structural conformation and equilibration of a protein during a simulation. Generally, if the RMSD value nears a fixed value, the protein has converged. Changes of 1-3 Å in RMSD values are acceptable for small, globular proteins. If the changes are much larger, there may be a large conformational change happening.

The Ligand RMSD (right Y-axis) plot reveals how stable a ligand is about the protein and its binding pocket. In the plot, "HTH fit Prot" indicates the RMSD of the ligand when the complex is first aligned to the protein backbone of the reference. If the value is considerably higher than the RMSD of the protein, then it is likely that the ligand has moved away from its initial binding site (Fig. 12).

The Root Mean Square Fluctuation (RMSF) is useful for characterizing local changes along the protein chain. The RMSF for residue i is:

$$RMSF_i \sqrt{\frac{1}{T}\sum_{i=1}^{T} < \left(\left(r_1'(t) - r_i(t_{ref}) \right) \right)^2 >}$$

where T is the trajectory time over which the RMSF is calculated, $tref$ is the reference time, r_i is the position of residue i; r' is the position of atoms in residue i after superposition on the reference, and the angle brackets indicate that the average of the square distance is taken over the selection of atoms in the residue.

In Fig. 12 of the plot, peaks indicate regions of the protein that experience the greatest degree of fluctuation during the simulation. It is typical to observe that the N- and C-terminal tails experience more fluctuation than other parts of the
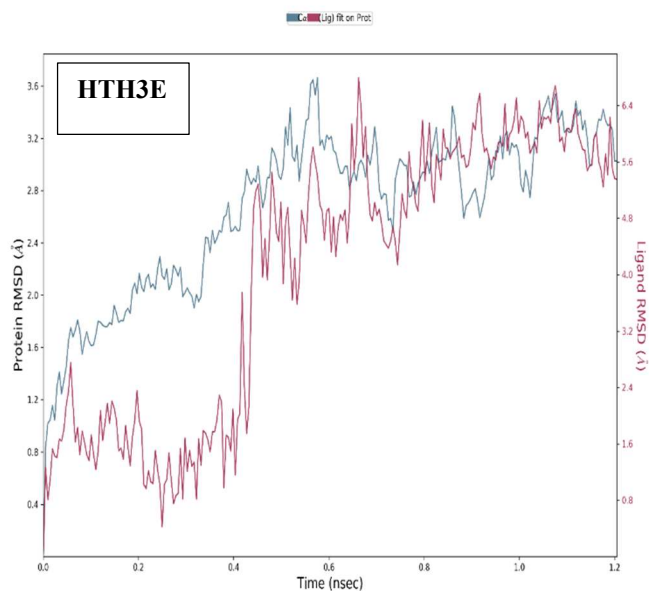

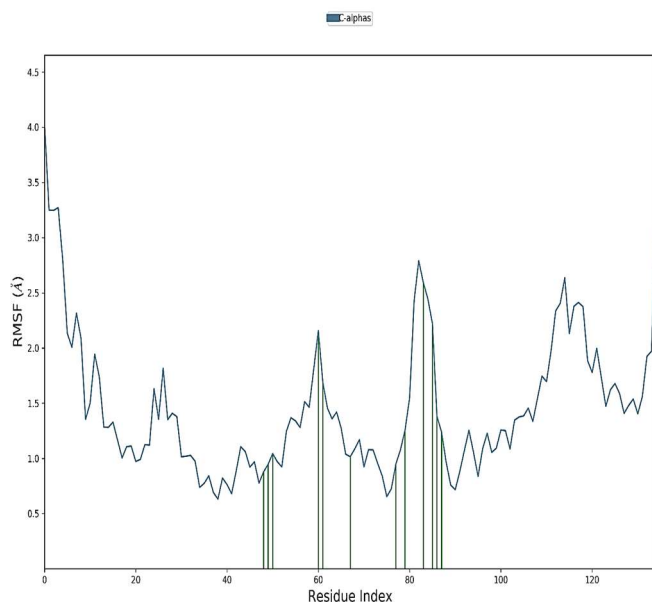**Fig. 11.** Plot of HTH3E-2BV6 receptor RMSD with Time (ns).

Fig. 12. A Plot RMSF of HTH3E-2BV6 protein against its Residue Index

protein. On the other hand, secondary structure elements, like alpha helices and beta strands, maintain a more rigid structure and thus fluctuate less than the surrounding loop regions.

The Ligand Root Mean Square Fluctuation (L-RMSF) is useful for characterizing changes in the ligand atom positions. The RMSF for atom *i* is:

$$RMSF_i \sqrt{\frac{1}{T}\sum_{i=1}^{T}\left(\left(r_1'(t)\right) - r_i\left(t_{ref}\right)\right)^2}$$

where *T* is the trajectory time over which the RMSF is calculated, t_{ref} is the reference time (usually for the first frame, and is regarded as the *zero* of time); *r* is the position of atom *i* in the reference at time t_{ref}, and *r′* is the position of atom *i* at time *t* after superposition on the reference frame. Ligand RMSF shows the ligand's fluctuations broken down by atom, corresponding to the 2D structure in the top panel (Fig. 13). The ligand RMSF provides information about how each ligand fragment interacts with the protein and its role in the binding event. The 'Fit Ligand on Protein' line in the bottom panel shows the fluctuations of the ligand relative to the protein backbone, which is measured for the ligand's heavy atoms. Conversely, the 'Ligand' line measures fluctuations of the ligand throughout the frames, by aligning on the reference frame of the ligand and calculating the RMSF values of its heavy atoms. These values effectively represent the internal atom fluctuations of the ligand.

Protein-Ligand Contacts

Protein-ligand interactions can be categorized into four different types: Hydrogen Bonds, Hydrophobic, Ionic, and Water Bridges. Each type contains more specific subtypes, which can be explored through the 'Simulation Interactions Diagram' panel. The normalized stacked bar charts show the amount of simulation time of each interaction subtype over the course of a trajectory. A value of 0.7 suggests that 70% of the time the interaction is maintained, while values over 1.0 suggest that more than one contact of the same subtype is formed with the ligand. Hydrogen Bonds (H-bonds) hold a significant role in ligand binding (Fig. 14) and are important to consider in drug design due to their strong influence on drug specificity, metabolization, and adsorption. The four subcategories of hydrogen bonds are backbone acceptor, backbone donor, side-chain acceptor, and side-chain donor. Figure 15 depicts a schematic of the detailed atom-level

interactions between a ligand and the protein residues. These interactions, which occur more than 30.0% of the time over the course of the selected trajectory from 0.00 to 10.00 nsec, are illustrated. Note: some residues may show atom-level interactions with this ligand surpassing 100%, since they may be interacting with the same atom in different ways.

CONCLUSION

Staphylococcus aureus is a commensal gram-positive bacterium that has captured the attention of the medical community for more than a century. It possesses many virulence factors, including toxins, superantigens, and proteins that are cell-wall associated. Molecular docking
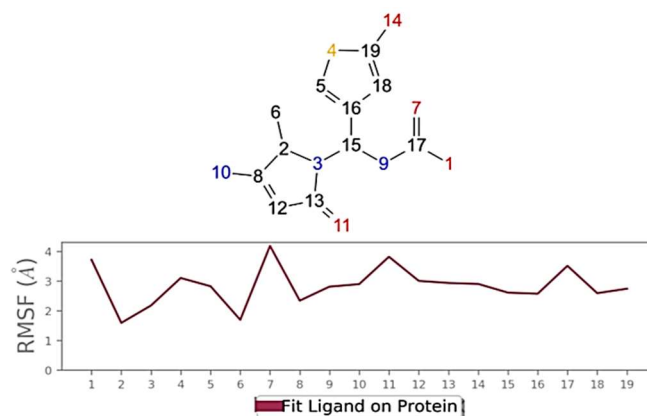

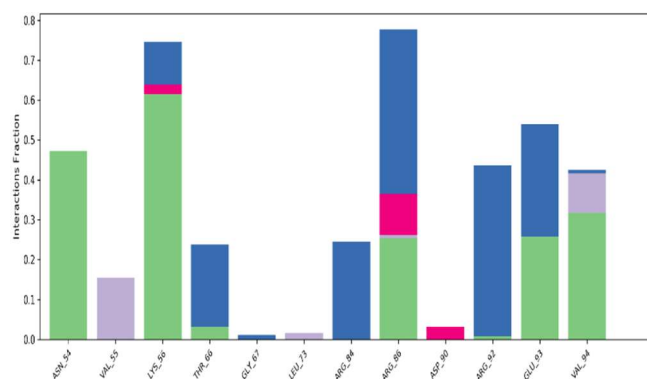**Fig. 13.** A Plot of Ligand HTH3E Root Mean Square Fluctuation (L-RMSF).

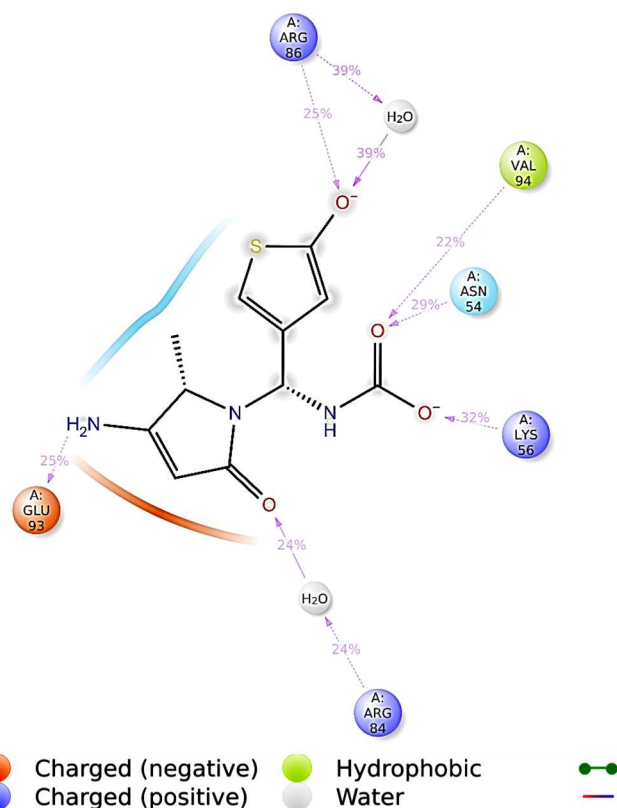**Fig. 14.** A Plot of Ligand HTH3E Interaction Fraction.

Fig. 15. A 2D ligand atom interactions with the protein residues.

presents a unique silico tool to assist drug design and discovery. However, beyond the applications for which it was originally developed, docking is now also widely employed to assist a variety of other drug discovery tasks, such as the identification of novel chemicals within large libraries of compounds, to perform in silico target fishing and profiling for drug repositioning, poly pharmacology prediction of advance and beyond, as described.

REFERENCES

[1] L.B. Rice, American Journal of Infection Control. 34 (2006) S11.

[2] F.C. Tenover, The American Journal of Medicine. 119 (2006) S3.

[3] U.G. Khan, *Developing a Lead Compound for the Inhibition of Bacterial DNA Gyrase*, 2016.

[4] J.G. Lombardino, J.A. Lowe, Nature Reviews Drug Discovery. 3 (2004) 853.

[5] M.D. Rawlins, Nature Reviews Drug Discovery 3 (2004) 360.

[6] E.-J. Yoon, M.Y. Lee, B.I. Choi, K.J. Lim, S.Y. Hong, D. Park, Antioxidants 9 (2020) 1111.

[7] M.T. Khan, M.J. Islam, A. Parihar, R. Islam, T.J. Jerin, R. Dhote, M.A. Ali, F.K. Laura, M.A. Halim, Informatics in Medicine Unlocked 24 (2021) 100578.

[8] A. Parihar, Z.F. Sonia, F. Akter, M.A. Ali, F.T. Hakim, M.S. Hossain, Computers in Biology and Medicine 145 (2022) 105468.

[9] D.E. Arthur, A. Uzairu, P. Mamza, E. Abechi, G. Shallangwa, Albanian Journal of Pharmaceutical Sciences 3 (2016) 4.

[10] D.E. Arthur, B.O. Elegbe, A.O. Aroh, M. Soliman, Bulletin of the National Research Centre 46 (2022) 1.

[11] P.R. Chen, T. Bae, W.A. Williams, E.M. Duguid, P.A. Rice, O. Schneewind, C. He, Nature Chemical Biology 2 (2006) 591.

[12] G. Šinko, Chemico-biological Interactions 308 (2019) 216.

[13] A.A. Naqvi, T. Mohammad, G.M. Hasan, M. Hassan, Current Topics in Medicinal Chemistry 18 (2018) 1755.

[14] D.E. Arthur, J.N. Akoji, R. Sahnoun, G.C. Okafor, K.L. Abdullahi, S.A. Abdullahi, C. Mgbemena, Bulletin of the National Research Centre 45 (2021) 1.

[15] L. Schrödinger, New York, NY, 2017.

[16] D. Shivakumar, E. Harder, W. Damm, R.A. Friesner, W. Sherman, Journal of Chemical Theory and Computation 8 (2012) 2553.

[17] D. Shivakumar, J. Williams, Y. Wu, W. Damm, J. Shelley, W. Sherman, Journal of Chemical Theory and Computation 6 (2010) 1509.

[18] U. Essmann, L. Perera, M.L. Berkowitz, T. Darden, H. Lee, L.G. Pedersen, The Journal of Chemical Physics 103 (1995) 8577.

[19] H.G. Petersen, The Journal of Chemical Physics 103 (1995) 3668.

[20] S. Jang, G.A. Voth, The Journal of Chemical Physics 107 (1997) 9514.

[21] G.J. Martyna, M.L. Klein, M. Tuckerman, The Journal of Chemical Physics 97 (1992) 2635.

[22] P.K. Patra, B. Bhattacharya, Physical Review E. 90 (2014) 043304.

[23] R. Salomon-Ferrer, D.A. Case, R.C. Walker, Wiley

Interdisciplinary Reviews: Computational Molecular Science 3 (2013) 198.

[24] A. Spasic, J. Serafini, D.H. Mathews, Journal of Chemical Theory and Computation 8 (2012) 2497.

[25] J. Kalayan, A. Chakravorty, J. Warwicker, R.H. Henchman, Proteins: Structure, Function, and Bioinformatics, 2022.

[26] J. Kalayan, R.H. Henchman, Physical Chemistry Chemical Physics 23 (2021) 4892.

[27] L. Pinzi, G. Rastelli, International Journal of Molecular Sciences 20 (2019) 4331.